Numerical Modeling of Crack-Defect Interaction

C. T. Liu*
Astronautics Laboratory (AFSC), Edwards Air Force Base, California 93523

An elastic analysis of the interaction between a main crack and defects was conducted using finite element methods. In the analysis, two different types of defects, voids, and damage were considered. The effects of the size, the location, and the number of voids, and, also, the intensity of damage on the Mode I stress intensity factor and the stress distribution near the crack tip region, were discussed.

Introduction

An important engineering problem in rocket motor structural design is evaluating structural integrity and reliability. It is well-known that structural strength may be degraded during its design life, due to mechanical or chemical aging, or a combination of these two aging mechanisms. Depending on the structural design, material type, service loading, and environmental condition, the cause and degree of strength degradation due to the different aging mechanisms differs. One of the common causes of strength degradation is the result of crack development in the structure. Depending on the cohesive strength of the solid propellant, the adhesive strength at the grain/liner/insulator/case interfaces, and the magnitude of the local stress in the material, cohesive failure (propellant cracking) may occur in the grain and/or adhesive failure (debond) may occur at interfaces. These two failure modes are commonly observed in solid rocket motors. Consequently, in evaluating the structural integrity of solid rocket motors, the effects of cohesive and adhesive fracture on their structural strength needs to be investigated.

When cracks occur, whether resulting from the manufacturing process or from applied service loads, the stress near the crack tip in a stressed body will be redistributed. Depending on the magnitude of the local stress and the local material strength, various types of defects can be developed near the crack tip region. Depending on its severity, defect near the crack tip can significantly affect the crack growth behavior. Therefore, in order to obtain a fundamental understanding of crack growth behavior in solid propellant, the interaction between the crack and the defect needs to be determined.

In this study, the TEXGAP-3D finite element computer code was used to determine the stress intensity factor at the crack tip, as well as the stress distributions in the vicinity of the crack tip in a centrally cracked sheet specimen. In the finite element analysis, two different types of defects were considered. For the first type of defect, it was assumed that the material in the neighborhood of the crack tip was damaged with different damage intensities, and the damaged materials were modeled by reducing the stiffness, or the modulus, of the material. For the second type of defect, it was assumed that different sizes of voids were developed at different locations near the crack tip, and the voids were modeled by setting the modulus of each element equal to 0.001 psi. In the analysis, a constant displacement, normal to the centerline of the crack, was applied at the boundary of the specimen, and a modulus of 500 psi was used for the undamaged material. The results of the finite element analysis were analyzed, and the effect of defect characteristics on the value of the stress intensity factor, as well as the stress distribution near the crack tip, were discussed. However, it should be pointed out that, although solid propellant may require large deformation and nonlinear representation, this study is intended to represent only an estimate of crack-defect interaction behavior.

Presented as Paper 89-2646 at the AIAA/ASME/SAE/ASEE 25th Joint Propulsion Conference, July 10–12 1989; received Dec. 5, 1989; revision received June 25, 1990; accepted for publication June 26, 1990.

*Materials Research Engineer.

Finite Element Analysis

The finite element method, one of the powerful methods of numerical stress analysis, is widely used both in research and in practical design. Using this method, a reasonably accurate approximate solution can be obtained for the stress distribution in a wide range of structures that have different material properties, complex geometries, and loading conditions. In this study, a linear elastic three-dimensional finite element computer code, known as TEXGAP-3D, was used to determine the stress intensity factor and the stress field in the centrally cracked sheet specimen. The TEXGAP-3D computer code contains conventional and reformulated elements, and can be used to analyze both compressible and incompressible materials. It also contains conventional crack elements derived from a hybrid displacement model. These crack elements, originally developed by Kathiresan and Atluri,[1] were developed for modeling compressible materials, therefore, they cannot be used to solve problems involving incompressible materials. However, for nearly incompressible materials, it has been determined that the finite element solution and the theoretical solution differ by 2.7% for a Poisson's ratio equal to 0.4999.[2] It has also been determined that the stress intensity factor is relatively insensitive to the Poisson's ratio when the Poisson's ratio is greater than 0.45, and is essentially unchanged when the Poisson's ratio is greater than 0.49. In addition, the finite element solution is also compared with the photoelastic solution for the cracked biaxial specimen obtained by Theiss.[3] It has been found that these two solutions differ by 1.45%. However, it should be pointed out that the photoelastic solution contains approximately 5% experimental scatter.

The specimen geometry shown in Fig. 1 was modeled as shown schematically in Fig. 2, taking full advantage of the symmetry of the problem by modeling only one-eighth of the specimen. Symmetry was imposed by using SLOPE boundary conditions (the SLOPE boundary condition produces the same effect as the rollers shown schematically in Fig. 2b) on ap-

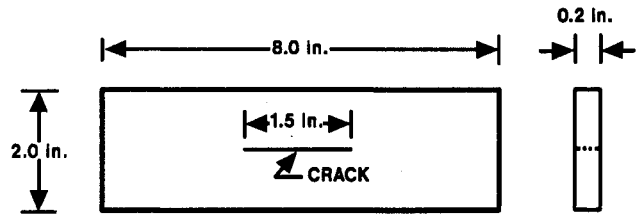

Fig. 1 Specimen geometry.

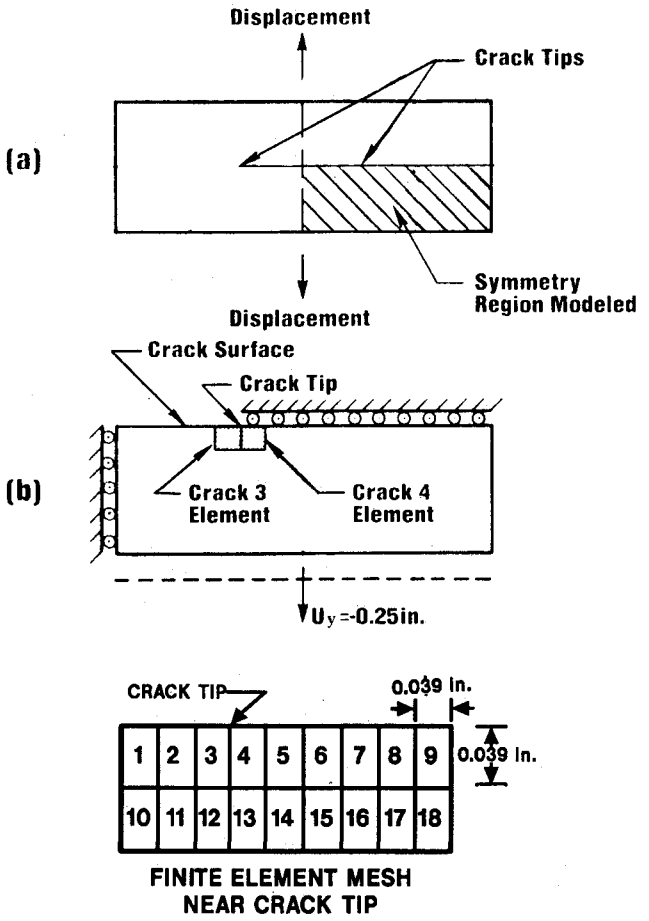

Fig. 2 Finite element model configuration.

propriate surfaces, as well as on the back face of the model (Fig. 2b). Displacement boundary conditions $U_Y = -0.25$ in. and $U_Z = U_X = 0$ were imposed on the lower boundary. The right boundary and the crack surface itself were modeled as free surfaces. CRACK 3 and CRACK 4, hybrid crack elements, were used at the crack tip to model the quadrant containing the free surface and the quadrant without a free surface, respectively. As mentioned previously, these crack elements are not reformulated for incompressibility, but they do provide a reasonably accurate solution.

In the finite element analysis, two different types of defects were considered. For the first type of defect, it was assumed that different sizes of voids were developed at different locations near the crack tip, and the voids were modeled by setting the modulus of each element equal to 0.001 psi. For the second type of defect, it was assumed that the material in the neighborhood of the crack tip was damaged, with different damage intensities. The damaged materials were modeled by reducing the stiffness, or the modulus, of the material. In the analyses, a Poisson's ratio of 0.4999 and a modulus of 500 psi were used for the undamaged material. For damaged materials, the modulus was set equal to 200 psi and 50 psi to simulate different intensities of damage near the crack tip. The results of the crack-defect interaction analysis are discussed in the following paragraphs.

Results and Discussion

Before we discuss the results of the crack-defect interaction analysis, we would like to discuss the change in local strains in the defect element prior to the formation of a void near the crack tip. In the analysis, the Young's modulus of element 14 (Fig. 2c) was reduced from 500 psi to 0.001 psi, with various values of modulus value in between. When the Young's modulus value is equal to 500 psi, the material is assumed to be in the undamaged state, whereas for the other values of the Young's modulus the material is assumed to be damaged. The results of the analysis, plotted with normal stress, normal strain, and shear strain as a function of the Young's modulus, are shown in Figs. 3 and 4. In Fig. 3, we note that the normal and the shear strains increase gradually as the Young's modulus is decreased from 500 psi to 20 psi and, then, a significant increase in normal and shear strains occurs as the Young's modulus is decreased from 0.1 psi to 0.001 psi. A similar trend was observed when the normal stress was plotted as a function of the Young's modulus, as shown in Fig. 4. This indicates that, in order to simulate a void, the modulus value should be set equal to or less than 0.001 psi. It also indicates that, prior to the formation of the void, large normal and shear strains occur at the void location. It is interesting to note that the value of K_I remains practically the same when the Young's modulus is varied from 500 psi to 20 psi, but is slightly increased when the Young's modulus is equal to 0.001 psi. This phenomenon occurs because 1) the void size is probably too small to affect the stress intensity factor and 2) the void is probably located in the low crack-void interaction zone. In order to get an insight into the crack-void interaction phenomenon, the effect of the size, the location, and the number of voids on the stress intensity factor was investigated. The results are discussed in the following paragraphs.

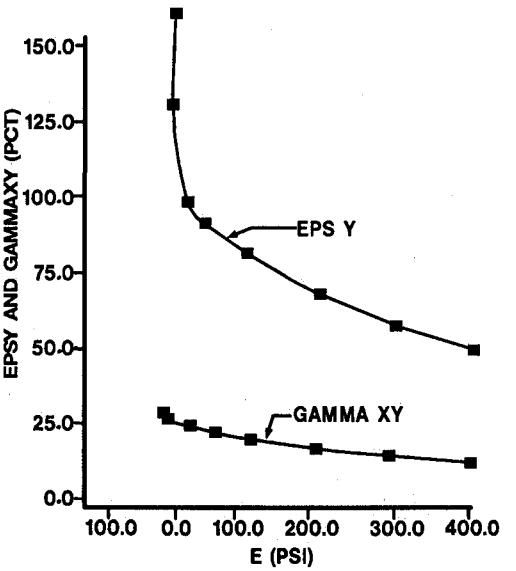

Fig. 3 Normal and shear strains vs Young's modulus.

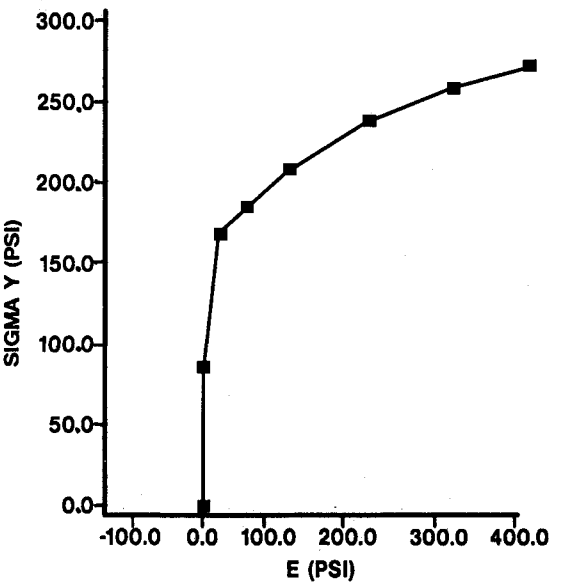

Fig. 4 Normal stress vs Young's modulus.

Table 1 Summary of the percentage change of K_I

Void element	K_I psi$\sqrt{\text{in.}}$	$\frac{K_I - K_{IO}}{K_{IO}}$[b], %
No void	168.78	0
——	172.72[a]	2.33
6	174.43	3.35
9	170.19	0.84
12	161.9	−4.07
6.12	166.26	−1.49
6.8	176.88	4.80
6.8, 12	169.3	0.31

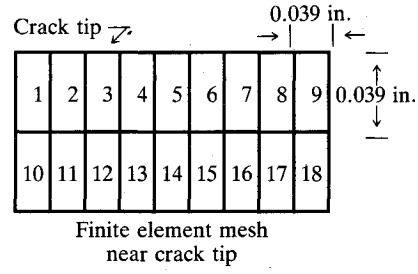

Finite element mesh near crack tip

[a]Experimental value. [b]K_{IO} = 168.78 psi$\sqrt{\text{in.}}$

Table 1 shows the summary of the percentage change of K_I as a result of crack-void interaction. From Table 1, we note that the value of K_I increases by 3.35% when a void is located at element 5, which is 0.059 in. ahead of the crack tip. The increase in K_I is decreased as the distance between the crack tip and the void is increased. When the distance between the crack tip and the 0.039 in. void reaches 0.315 in., there is a negligible effect of the void on the value of K_I at the crack tip. However, when a 0.118 in. void is located directly at 0.039 in. and 0.079 in. ahead of the crack tip—the value of K_I is increased by 18.98% and 9.84%, respectively. This indicates that, for a given distance ahead of the crack tip, a large void will induce a relatively large increase in the value of K_I. This also indicates that there exists a limiting distance ahead of the crack tip beyond which no crack-void interaction will take place. The intensity of the interaction and the size of the interaction zone will increase as the size of the void increases. Referring back to Table 1, when a 0.039 in. void is located at element 12, the value of K_I is decreased by 4.07%. It is interesting to point out that when two voids, one located at element 6 and the other located at element 12, exist near the crack tip, the value of $\Delta K/K_{IO}$% is equal to −1.49%, which is close to the sum of the two values of $\Delta K/K_{IO}$%, corresponding to the two voids when they exist separately. This implies that within the crack-void interaction zone, the interaction between the crack tip and isolated voids of the same size appears to follow a simple additive rule, or a linear cumulative interaction rule. In other words, it appears that the total effect of crack-void interaction induced by multiple isolated voids of the same size is approximately equal to the sum of the interaction effects induced by the individual void. In order to verify the validity of the linear cumulative interaction rule, additional crack-void interaction analyses of different void distributions need to be conducted.

Figure 5 illustrates the effect of a 0.039 in. void behind the crack tip on the interaction of the crack and a 0.118 in. void ahead of the crack tip. For this example, both the 0.039 in. void and the 0.118 in. void are located 0.039 in. below the crack plane and the tip of the 0.118 in. void is aligned with the crack tip. From Fig. 5, the stress intensity factor is 202.48 psi$\sqrt{\text{in.}}$ when there is no void behind the crack tip. However, when a 0.039 in. void is located 0.039 in. behind the crack tip, the stress intensity factor is 188.41 psi$\sqrt{\text{in.}}$ As the distance between the crack tip and the 0.039 in. void is increased to 0.079 in., the stress intensity factor is 199.28 psi$\sqrt{\text{in.}}$ On the other hand, when the 0.039 in. void joins the 0.118 in. void to form a 0.157 in. void, the stress intensity factor is 156.1 psi$\sqrt{\text{in.}}$, which is a 7.51% reduction from the case in which no void exists. This indicates that the 0.157 in. void produces a shielding effect on the main crack. It is interesting to note that a comparison of the 0.157 in. void case with the two cases, in which the 0.039 in. void and the 0.118 in. void exist separately, indicates that the linear cumulative interaction rule does not apply to the case when the two voids join together.

Having discussed the effect of crack-void interaction on the stress intensity factor, we will proceed to discuss the results

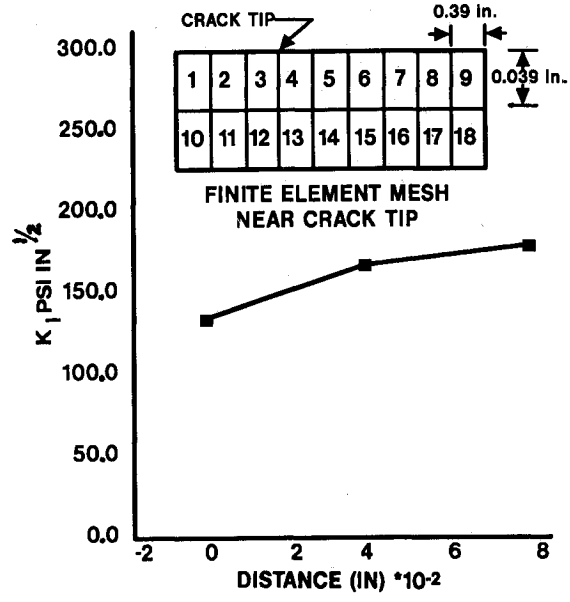

Fig. 5 Stress intensity factor vs void distance behind crack tip.

of crack-damage interaction analysis in the following paragraph.

Table 2 shows the summary of the results of the crack-damage interaction analysis. From Table 2, it is seen that the modulus of the two crack tip elements (elements 3 and 4) has a significant effect on the value of K_I. When the modulus of the two crack tip elements is reduced from 500 psi to 50 psi, the value of K_I is reduced from 168.78 psi$\sqrt{\text{in.}}$ to 42.62 psi$\sqrt{\text{in.}}$, a 74.75% reduction. It is interesting to note that the change of modulus of the elements surrounding the two crack tip elements has a negligible effect on the value of K_I. In addition, when a 0.118 in. void exists at a distance of 0.079 in. directly ahead of the crack tip, a reduction of the modulus of the two crack tip elements from 500 psi to 50 psi also results in a reduction of the value of K_I from 177.9 psi$\sqrt{\text{in.}}$ to 44.37 psi$\sqrt{\text{in.}}$ A comparison of the various crack-defect interaction cases shown in Table 2 reveals that, when the modulus of the two crack tip elements is equal to 50 psi, and if no large void exists below the crack tip, the existence of additional defects near the crack tip region has a negligible effect on the value of K_I. This suggests that the linear cumulative interaction rule mentioned earlier does not apply to these cases. It also suggests that the damage state on the material in the immediate neighborhood of the crack tip controls the value of K_I.

In the above paragraphs, the discussion was centered on the effect of defects, voids, and damage on the value of K_I at the crack tip. It was found that, depending on the size and location of the void, the value of K_I can be increased or decreased. It was also found that the magnitude of K_I is highly dependent on the damage state in the immediate vicinity of the crack tip, and is relatively insensitive to the damage state away from the crack tip. Depending on the intensity of the damage at the crack tip, the magnitude of K_I can be signifi-

Table 2 Summary of results of crack-defect interaction analysis

Element modulus, psi	Void element	K_T psi$\sqrt{\text{in.}}$
E_3[a] = E_4 = 50	No void	42.62
	6, 12	38.06
	6, 12, 13	24.98
	6, 12, 13, 14	26.41
	7, 8, 9	44.37
$E_3 = E_4 = 50$ $E_{12} = E_{13} = E_{14}$ $= E_5 = 200$	7, 8, 9	45.80

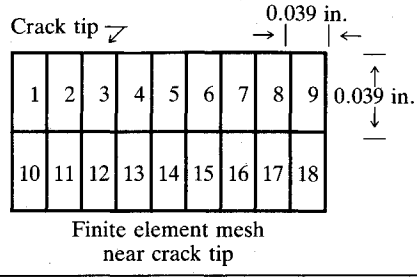

Finite element mesh near crack tip

[a]E_i = Young's modulus of ith element.

cantly reduced, and the crack tip can be significantly blunted. Since the crack growth behavior is controlled by the local stress near the crack tip, an increase (decrease) in the magnitude of K_I will also result in an increase (decrease) in the crack growth rate. If the magnitude of K_I drops below a threshold value, the crack may stop growing. Based on this discussion, it is expected that the existence of local defects near the crack tip is a contributing factor to the stable and fluctuating crack growth behavior in solid propellants.

As discussed in the previous paragraphs, the existence of defects near the crack tip may result in crack tip blunting. The blunting of the crack tip will relax the high local stress, resulting in a high resistance to propagation of the crack. Under this condition, in order to get insight into the crack-growth behavior, it is necessary to investigate the effect of local defects near the crack tip on the stress state in the neighborhood of the crack tip. The results of the investigation are discussed in the following paragraphs.

A plot of the normal stress, σ_y, along the crack plane for various crack-void interaction cases is shown in Fig. 6. For comparison purposes, the void-free case, denoted as the baseline case. From this figure, it can be seen that the effect of the presence of voids on the distribution of σ_y ahead of the crack tip depends on the size, the location, and the number of voids. Because of the complex interaction mechanisms in the highly interactive region, which is the region between the crack tip and the left side of the void tip, there is no consistent trend as far as the effect of the void on the value of σ_y is concerned. A comparison between the crack-void interaction cases and the baseline case reveals that the existence of two voids at elements 6 and 12, or the existence of three voids at elements 6, 12, and 13, increases the value of σ_y. On the other hand, a significant reduction in σ_y in the high-interaction region occurs when four voids exist at elements 6, 12, 13, and 14. Figure 6 also shows that the existence of voids consistently increases the value of σ_y in the low-interaction region, which is the region to the right of the right-side void tip. It is interesting to point out that, unlike in the high interaction region, the existence of voids at elements 6, 12, 13, and 14 induces the highest value of σ_y in the low-interaction region. For the three crack-void interaction cases considered, the magnitudes of σ_y decrease as the distance from the right side of the void tip increases, and eventually these magnitudes equal that of σ_y of the baseline case at different distances from the right-side void tip. These different distances define the boundaries of the low-interaction regions, which depend on the void size; the larger the void the larger the low-interaction region.

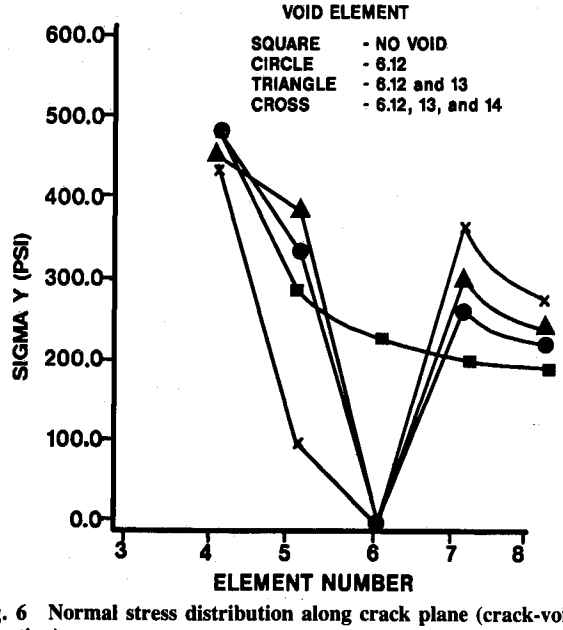

Fig. 6 Normal stress distribution along crack plane (crack-void interaction).

Having discussed the effect of crack-void interaction on the distribution of σ_y near the crack tip, we proceed with a discussion on the effect of damage at the crack tip, and its interaction with voids on the distribution of σ_y near the crack tip. Figure 7 shows the effect of the reduction of the modulus of the two crack tip elements on σ_y near the crack tip region. By comparing the two curves shown in Fig. 7, we note that, at 0.020 in. ahead of the crack tip, the reduction of the modulus of the two crack tip elements from 500 psi to 50 psi reduces the magnitude of σ_y from 480 psi to 119.4 psi, a 75.12% reduction. However, the reduction of the modulus of the two crack tip elements increases the magnitude of σ_y by 20.22% at a point 0.059 in. ahead of the crack tip. An examination of the two curves shown in Fig. 7 reveals that these two curves are approximately parallel at 0.059 in. ahead of the crack tip. This implies that a reduction of the modulus in a small region at the crack tip causes a shift in the distribution curve of σ_y to the same small distance ahead of the crack tip. In other words, the effect of damage in a small region at the crack tip is equivalent to increasing the crack length by a small amount. This is similar to the correction of the crack length for small scale yielding proposed by Irwin[4] in his study of the effect of a small plastic zone at the crack tip on the stress distribution head of the trip.

The effect of the interaction of voids with a damaged crack tip on the distribution of σ_y near the crack tip region is shown in Fig. 8. From Fig. 8, when the modulus of the two crack tip elements is equal to 50 psi, the magnitudes of σ_y at the centroid of element 4, which is 0.02 in. ahead of the crack tip, are relatively small. A comparison with the no-void case shows that the existence of voids induces a smaller normal stress σ_y. However, a significant increase in σ_y occurs at a point 0.059 in. ahead of the crack tip, when voids exist either at elements 6 and 12 or at elements 6, 12, and 13. On the other hand, when voids exist at elements 6, 12, 13, and 14, the magnitude of σ_y only increases slightly. Figure 8, also shows that, in the low-interaction region, the existence of voids consistently induces a higher magnitude of σ_y, with the largest void inducing the highest σ_y. The effect of the reduction of the modulus of the two crack tip elements on the results of crack-void interaction can be evaluated by comparing Fig. 6 with Fig. 8. From these two figures, we see that the reduction of the modulus of the two crack elements significantly reduces

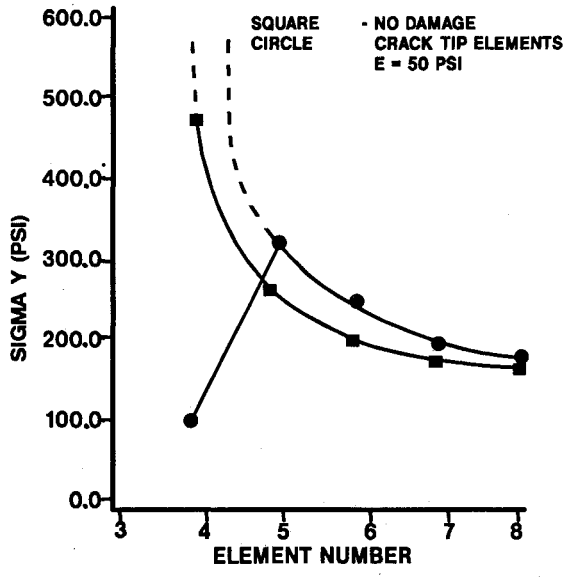

Fig. 7 Normal stress distribution along crack plane.

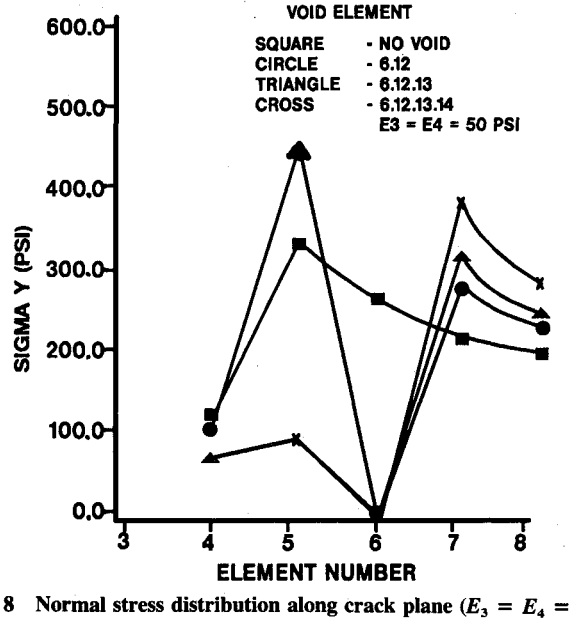

Fig. 8 Normal stress distribution along crack plane ($E_3 = E_4 = 50$ psi).

σ_y at element 4 and significantly increases σ_y at element 5 when voids exist either at elements 6 and 12 or at elements 6, 12, and 13. However, when voids exist at elements 6, 12, 13, and 14, the reduction of the modulus of the two crack tip elements 3 and 4 induces a negligible effect on σ_y at element 5. This implies that, when a large void exists 0.039 in. below the crack tip, it will produce a shielding effect on the crack tip, and this effect appears to be insensitive to the modulus of the two crack tip elements. Referring back to Fig. 6 and Fig. 8, we also note that the reduction of modulus of the two crack tip elements induces a higher σ_y in the low-interaction region, resulting in a larger size or low-interaction region.

Figure 9 shows the distribution of σ_y along the crack plane when a 0.118 in. long void (elements 7, 8, and 9) exists 0.118 in. ahead of the crack tip, which is surrounded by two layer elements with different moduli. The inner layer elements, which consist of the two crack elements 3 and 4, have a modulus of 50 psi, whereas the outer layer elements, which consist of elements 5, 12, 13, and 14 have a modulus of 200 psi. According to Fig. 9, the magnitudes of σ_y at 0.02 in. ahead of the crack tip are almost the same, regardless of whether the outer layer and/or the 0.118 in. void exist or not. However, the magnitudes of σ_y at elements 5 and 6 depend on the distribution of the modulus of the elements in the neighborhood of the crack tip and on whether there is a 0.118 in. void or not. This implies that only the damage intensity at the immediate vicinity of the crack tip has a significant effect on the stress intensity factor at the crack tip.

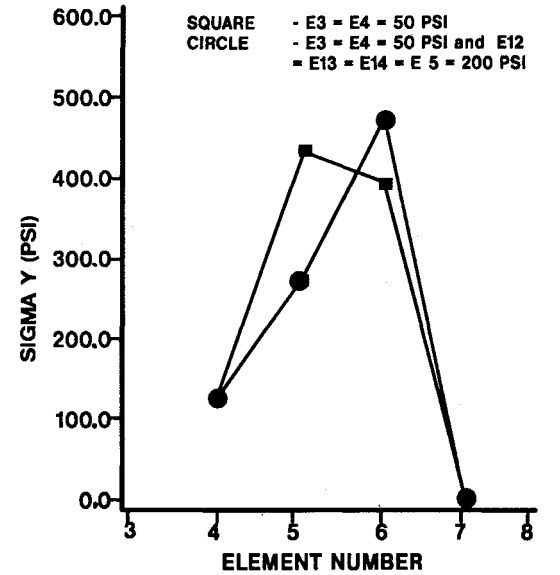

Fig. 9 Normal stress distribution along crack plane ($E_3 = E_4 = 50$ psi, $E_5 = E_{12} = E_{13} = E_{14} = 200$ psi).

Conclusions

In this study, an elastic analysis of crack-defect interaction was conducted using finite element methods. In the analysis, two types of defects, voids and damage, were considered. The void was modeled by setting the Young's modulus of the void element equal to 0.001 psi, and the damaged element was modeled by reducing the Young's modulus of the element. The effects of the size, the location, and the number of voids, as well as the damage distribution on the Mode I stress intensity factor and the stress distribution near the crack tip region, were investigated. The results of the analysis reveal that, depending on the size, location, and number of voids, the interaction between the crack and the voids can increase or decrease the value of the stress intensity factor and can significantly affect the stress distribution in the high-interaction, as well as the low-interaction, region. The size of the low-interaction region increases with increasing void size. The results of the analysis also reveal that the stress intensity factor at the crack tip and the stress distribution in its immediate vicinity are highly dependent on the damage intensity in that vicinity, and are relatively insensitive to the damage state away from the crack tip. However, the stress distribution in a region away from the crack tip will be affected by the damage state in that region. Since crack-growth behavior is controlled by local stress near the crack tip, the fluctuation of stress and the damage toughening effect induced by crack-defect interaction are believed to be contributing factors to stable and fluctuating crack growth in solid propellants.

References

[1]Kathiresan, K., and Atluri, S. N. *Three-Dimensional Homogeneous and B-Material Fracture Analysis for Solid Rocket Motor Grains by a Hybrid Displacement Finite Element Method*, AFRPL-TR-78-65, 1978.

[2]Liu, C. T., Jacobsen, A. E., and Thrasher, D. I., "Effect of Poisson's Ration on Stress Intensity Factors," *1982 JANNAF Structures and Mechanical Behavior Meeting*, CPIA Publication 368, Oct. 1982, pp. 379–390.

[3]Theiss, T. J., "Preliminary Investigation into the Cracking of Polyurethane," Master's Thesis, Virginia Polytechnic Inst. and State Univ., Blacksburg, VA, 12 June 1987.

[4]Irwin, G. R., "Plastic Zone Near Crack and Fracture Toughness," Sagamore Conf., Syracuse University Press, Syracuse University, N.Y. P.P. IV-63, 1960.